JOURNAL OF THE KOREAN ASTRONOMICAL SOCIETY
40: 147 ~ 151, 2007

ADVANCES IN CIRCUMSTELLAR MEDIUM EVOLUTION

GUILLERMO GARCÍA-SEGURA
Instituto de Astronomía, Universidad Nacional Autónoma de México
Apdo. Postal 877, 22800 Ensenada, B.C., Mexico
E-mail: ggs@astrosen.unam.mx
(Received November 28, 2007; Accepted December 7, 2007)

ABSTRACT

We discuss recent advances in hydrodynamical computations of the circumstellar medium, which are useful to understand some features observed in long gamma ray bursts

Key words : stars: evolution — circumstellar matter — hydrodynamics — ISM: bubbles

I. INTRODUCTION

The evolution of a star, imprinted in its location on the Hertzpung-Rusell diagram (HRD) is a basic key to understand the formation and evolution of structures in the circumstellar medium (CSM), such as bubbles and swept-up shells. When stars have high temperatures they are relatively compact (small radius $\sim R_\odot$), and their wind velocities ($\propto$ escape velocities) are of the order of $\sim 10^3$ km s^{-1} . On the other hand, when stars have low temperatures, their radii are large ($\sim 10^2 - -10^3 R_\odot$), and their wind velocities (escape velocities) are relatively small, of the order of $\sim 10^1 - -10^2$ km s^{-1} . Then, every time that a slow wind evolves into a fast wind, a swept-up shell is formed.

The theory of wind blown bubbles is well represented by the Weaver's et al. (1977) paper (30 years of success), and it was thought for main sequence (MS) stars with fast winds sweeping up the ISM. Their analytical solutions gives a good insight for the dynamics of the interaction MS $\rightarrow$ ISM, assuming that the MS sequence wind is constant (which is a good approximation) . However, most nebulae surrounding stars do not belong to this scenario (only a few of them, such as the case of the bubble nebula NGC 7635), and post-MS evolution has to be taken into account, with time dependent winds.

An effort to couple stellar evolution calculations with the CSM evolution by using hydrodynamical simulations have been made for several stellar models: 12 $M_\odot$ (Chita et al. 2007), 20 $M_\odot$ (van Marle et al. 2008), 23, 28, 29, 30 and 33 $M_\odot$ (Pérez-Rendón et al. 2008), 35 and 60 $M_\odot$ (García-Segura et al. 1996ab), and for low and intermediate stellar masses, 1, 1.5, 2, 2.5, 3.5 a 5 $M_\odot$ (Villaver et al. 2002ab). All these studies follow the same scheme which is shown in Figure 1. Although this is still premature, the goal of this scheme is to provide a feedback for the stellar evolution calculations, denoted by the question mark in Figure 1.

Corresponding Author: G. García-Segura

In the rest of this article, we will discuss only specific points that are of interest. The reader is encouraged to read above references for further insight into this problem.

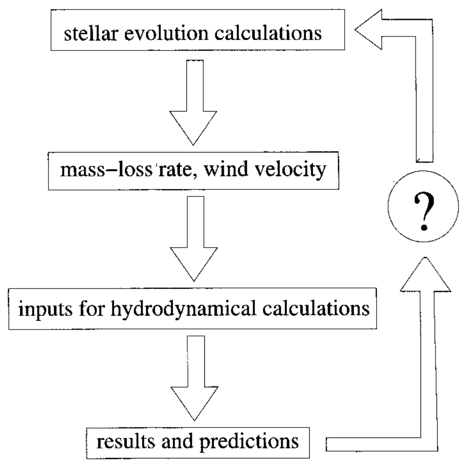

Fig. 1.— Logical scheme in CSM computations

II. RED SUPER GIANT SHELLS

Although red super giant (RSG) shells, formed by the collision between RSG winds and MS pressurized bubbles, have been predicted by hydrodynamical simulations, there is not yet any observational confirmation of their existence. There is only one controversial case, HD 179821 (Jura & Werner 1999), but other authors believe that this is an AGB at 1 kpc, instead of a RSG a 3 kpc. The predicted shells should have sizes between 3 and 10 pc in radius, with low temperatures, probably emitting only in infrared. Their sizes on the sky would be of the order of several arcmin, so the confusion with the background is a problem to consider. Since these shells are dust rich, observations based on extinction methods are also something to study.

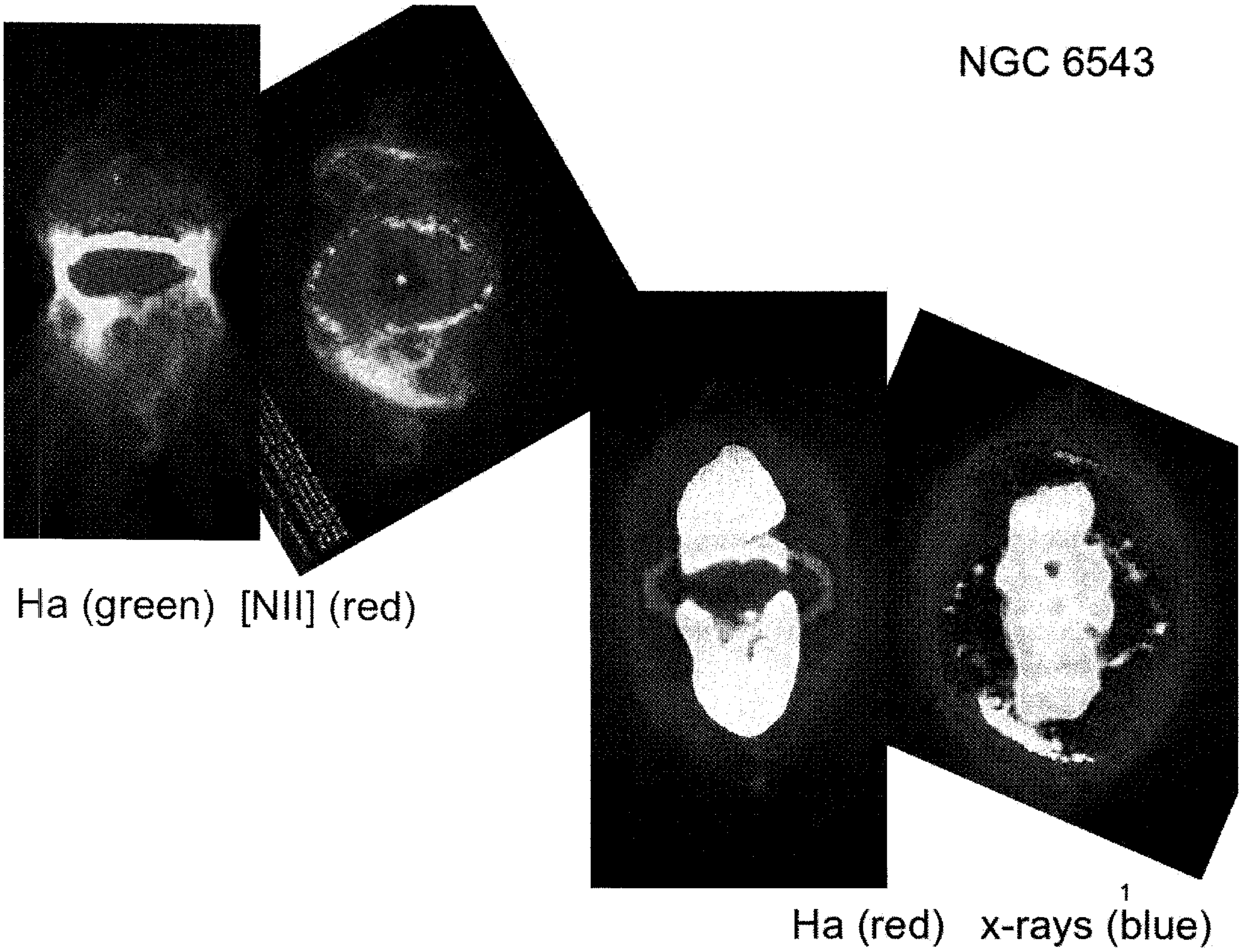

Fig. 2.— An example of a 3-D MHD simulation compared with the HST and Chandra images of NGC 6543

III. WOLF-RAYET BUBBLES

The bubbles surrounding Wolf-Rayet (WR) stars are the best laboratories to study the predictions made by the wind blown bubble theory. The analytical solutions by García-Segura & Mac Low (1995), which are an extension of Weaver's et al. (1977) solutions for power laws, give a good insight for the dynamics of the interaction WR $\rightarrow$ RSG. X-ray observations proved the existence of 10^6 K plasma inside the bubbles (NGC 6888 Bochkarev 1988; S308 Chu et al. 2003), as well as UV observations confirmed the existence of conduction fronts (Boroson et al. 1997).

Recently, new discoveries in long gamma ray bursts, in particular, the detection of interstellar absorption lines on top of the emission from the afterglow, have turn the attention again into these WR bubbles. The observed groups of lines, with blue shifted velocities up to $\sim$ 3000 km s^{-1} respect to the afterglow, are thought to originate in the WR wind progenitor and in previous interactions of the CSM (see van Marle et al. 2005 for further details and references therein). Thus, these observations show, in detail, the whole previous evolution of the CSM around long gamma ray burst progenitors.

There is still a dynamical problem with wind blown bubbles, in particular with WR bubbles. If we use the mechanical luminosity (either theoretical or from observations) as input to explain the dynamics, the swept-up shells would expand faster by a factor of 2, the expected x-ray luminosities and the O VI column densities would be larger by a factor of 10. However, if we consider as inputs the expansion velocity of the swept-up shell and the swept-up mass, the expected x-rays and OIV column densities are well predicted, but the needed mechanical luminosity is a factor of 10 smaller. Thus, there is still a controversy about the measurements of the mass loss rates for WR stars (see for example García-Segura & Mac Low 1995 for the case of the WR bubble NGC 6888).

IV. THE Ω LIMIT

If bipolarity comes from the stellar rotation and the loss of angular momentum, one can learn from the case of the most massive stars and their associated nebulae. In the Hertzsprung-Russell diagram, luminous blue variables (LBVs) stars like η Car lie close to the upper limit in temperature and luminosity beyond which no normal stars are observed (the Humphreys-Davidson Limit), near the location of the Eddington limit.

A massive star expanding at a constant luminosity L would —*in the non-rotating case* — reach the Eddington limit due to an opacity increase in the surface layers. The Eddington limit is reached when $\Gamma = L/L_{\rm Edd} = 1$, where the Eddington luminosity is $L_{\rm Edd} = 4\pi cGM/\kappa$, with c the speed of light, M and L the mass and luminosity of the star, and κ the opacity at the stellar surface. Note that when $\Gamma \to 1$, the escape velocity $v_{\rm esc} = [(1-\Gamma)2GM/R]^{1/2} \to 0$. This implies a very slow wind velocity ($\simeq 0$) at the Eddington limit. Thus, when a star passes through a close approach to the Eddington limit, its stellar wind will follow a *fast—slow—fast* sequence. If we now include rotation, the critical rotational velocity also follows the same behavior. The combination of radiation pressure and centrifugal force exceeds surface gravity at the equator when $v_{\rm crit} = [(1-\Gamma)GM/R]^{1/2}$, and $v_{\rm crit} \to 0$ when $\Gamma \to 1$. However, given that the rotational velocity $v_{\rm rot}$ can be small but is always different from zero, critical rotation occurs *before* the Eddington limit is reached. This is the so called *Ω limit* (Langer 1997). Winds with mass loss rates large enough to halt and reverse the stellar expansion are thought to occur when $\Omega = v_{\rm rot}/v_{\rm crit}$ approaches unity (Friend & Abbott 1986). Thus, rotationally driven outflows will always occur before the star reaches its Eddington limit.

The Ω limit, which is actually the Eddington limit including the stellar rotation, has been successful in explaining bipolar nebula around post-MS objects, such as η Carina and other LBVs (Langer et al.1999). Recently, new studies of stars at blue loops, such as the 12 $M_\odot$ model discussed in Chita et al.(2007) reveals that stars at this stage can achieve critical rotation, explaining bipolar nebulae around blue super giants such as Sher 25. But this is not the only place where stars can achieve critical rotation, actually stars at the end of MS (H-core burning) and at the end of He MS phase (He-core burning) (van Marle et al. 2008) can achieve critical conditions when stars undergo core collapses.

V. MAGNETIC FIELDS

The inclusion of a weak magnetic field in a line-drive wind results in a very powerful tool to understand many of the dynamical processes involved in WR bubbles and planetary nebulae (PNs). Chevalier & Luo (1994) made thin-shell, semi analytical solutions to explore the effects of a rotating star with a magnetized wind on the formation of aspherical bubbles. Following this scheme, Różyczka & Franco (1996) and García-Segura et al. (1999a), performed 2-D MHD simulations of magnetized winds in cylindrical and spherical calculations, respectively, showing that magnetic tension may indeed be responsible for the generation of jets in PNs. García-Segura (1997) presented full 3-D MHD models of PNs where jets and ansae are convincingly reproduced as the result of magnetic collimation of the post-AGB wind. An example is shown in Figure 2, which shows that MHD simulations can be extremely successful in reproducing all kind of complicated features in PNs, such as the case of NGC 6543, a bipolar nebula, with an internal elliptical bubble, with precessing jets and ansae.

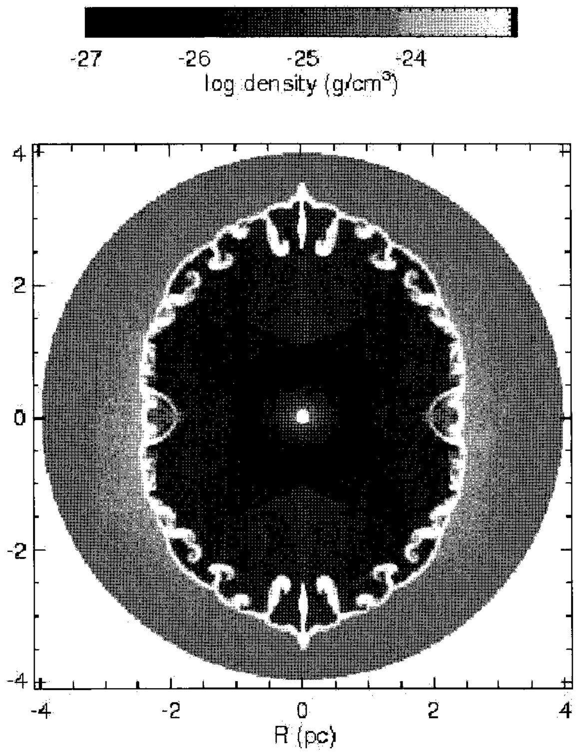

Fig. 3.— Magnetized WR bubble with $\sigma = 0.00035$

Since MHD computations are successful, for example in PNs, we can make predictions for other kind of objects, such as WR bubbles and long gamma ray burst (LGRBs) progenitors. The key parameter is σ, which is the ratio of the magnetic energy over the kinetic energy in the wind, defined as:

$$\sigma = \frac{B^2}{4\pi\rho v_\infty^2} = \frac{B_s^2 R_s^2}{\dot{M}\ v_\infty}\left(\frac{v_{\rm rot}}{v_\infty}\right)^2 \qquad (1)$$

Note that σ is very sensitive with the rotation velocity, and this is the point in the present discussion. It is easy to produce models that fit with galactic WR bubbles like NGC 6888, with very small values for σ,

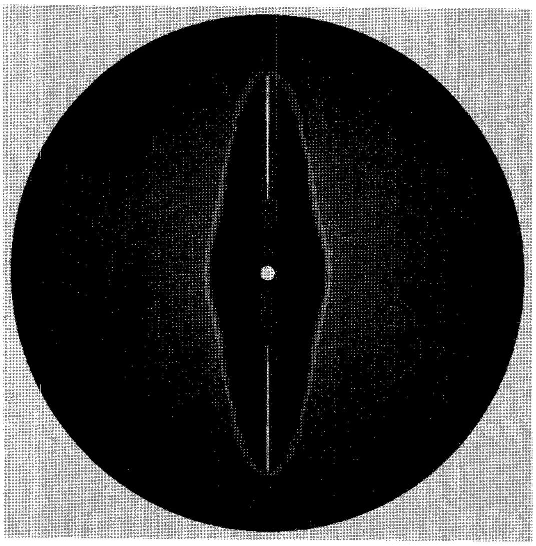

Fig. 4.— Magnetized WR bubble with $\sigma = 0.01$

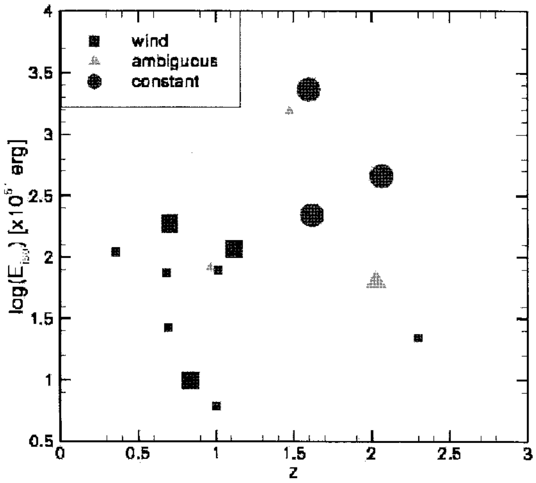

Fig. 5.— Type of CSM reveled by afterglows from LGRBs over the redshift-isotropic energy space (van Marle et al. 2006)

as it is shown in Figure 3 (García-Segura et al. 1999b). However, just increasing slightly the value of the rotational velocity, σ can be incremented to values of 0.01, like the model shown in Figure 4. By doing this, we obtained an elongated bubble, that probably does not match with galactic observations, but it has an important feature in the context of LGRBs. This is the position of the reverse shock at the polar regions, which is the region that is going to decelerate the relativistic jet coming from the LGRB. Note that the reverse shock in the magnetized model is much closer to the star (compare Figure 4 with 3), almost a factor of 10. Figure 4 does not have labels, but the spatial dimension is similar to Figure 3. Note that after crossing the reverse shock in the polar direction, the density is rather constant, with larger values than the rest of the bubble due to the hoop stress pilling up. There is a controversy about why some LGRB jets appears to slow down in a constant medium (van Marle et al.2006 and references there in), and others in a free expanding wind like r^{-2}. This is illustrated in Figure 5. The LGRBs that show a constant medium around, appears to be at higher redshift, while the one that decelerate in a free wind appears to be closer to us. Since there is a correlation between redshift and metallicity, stars at higher redshift would have lower metallicities. But this also means that, the mass-loss rate from these stars would be smaller, and so the angular momentum lost in the winds. Thus, this scenario favors the idea that these stars do not slow down their rotational velocities during the evolution so effective as the stars with higher metallicities. From here, it is expected that, at lower metallicities (higher redshift), the MHD effects, and the importance of σ could be notorious, giving a natural explanation for Figure 5. The larger luminosity is also correlated with the larger densities closer to the central stars.

ACKNOWLEDGEMENTS

G.G.-S. thanks the L.O.C. of "The 4th Korea-Mexico Joint workshop on Astrophysics: Interstellar Medium", KASI, KOSEF and CONACyT for all the effort made in this excellent conference. G.G.-S. also thank Michael L. Norman and the Laboratory for Computational Astrophysics for the use of ZEUS-3D. All computations were performed at Instituto de Astronomía-Universidad Nacional Autónoma de México. This work has been partially supported by grants from DGAPA-UNAM (IN130698, IN117799 & IN114199) and CONACyT (32214-E).

REFERENCES

Bochkarev, N. G. 1988, X-ray emission from the ring nebula NGC6888, Nature, 332, 518

Boroson, B., McCray, R., Clark, C. O., Slavin, J., Mac Low, M., Chu, Y., & Van Buren, D. 1997, An interstellar conduction front within a Wolf-Rayet ring nebula observed with the Goddard high resolution spectrograph, ApJ, 478, 638

Chevalier, R. A. & Luo, D. Magnetic shaping of planetary nebulae and other stellar wind bubbles, 1994, ApJ, 421, 225

Chita, S. M., van Marle, A. J., Langer, N., & García-Segura, G. 2007, The evolution of circumstellar medium around rotating massive stars, RMxAC, 30, 80

Chu, Y.-H., Guerrero, M. A., Gruendl, R. A., García-Segura, G., & Wendker, H. J. 2003, Hot gas in the circumstellar bubble S308, ApJ, 599, 1189

Friend, D. B., & Abbot, D. C. 1986, The theory of radiatively driven stellar winds. III - Wind models with finite disk correction and rotation, ApJ, 311, 701

García-Segura, G. 1997, Three-dimensional magnetohydrodynamical modeling of planetary nebulae: The formation of jets, ansae, and point-symmetric nebulae via magnetic collimation, ApJ, 489, L189

García-Segura, G., Langer, N., Różyczka, M., & Franco, J. 1999a, Shaping bipolar and elliptical planetary nebulae: Effects of stellar rotation, photoionization heating, and magnetic fields, ApJ, 517, 767

García-Segura, G., Langer, N., Rzyczka, M., Franco, J., & Mac Low, M.-M. 1999b, Hydrodynamics of ring nebulae: magnetic vs. non-magnetic hydro-models, IAU Symp. 193, 325

García-Segura, G., Langer, N., & Mac Low, M.-M. 1996b, The hydrodynamic evolution of circumstellar gas around massive stars. II. The impact of the time sequence O star → RSG → WR star, A&A, 316, 133

García-Segura, G., & Mac Low, M.-M. 1995, Wolf-Rayet Bubbles. I. Analytic Solutions, ApJ, 455, 145

García-Segura, G., Mac Low, M.-M., & Langer, N. 1996a, The dynamical evolution of circumstellar gas around massive stars. I. The impact of the time sequence Ostar → LBV → WR star, A&A, 305, 229

Langer, N. 1997, The Eddington limit in rotating massive stars, ASPC, 120, 83

Langer, N., García-Segura, G., & Mac Low, M.-M. 1999, Giant outbursts of luminous blue variables and the formation of the homunculus nebula around eta Carinae, ApJ, 520, L49

Jura, M., & Werner, M. W. 1999, The detached dust shell around the massive star HD 179821, ApJ, 525, L113

Pérez-Rendón, B., García-Segura, G., & Langer, N. 2008, in preparation

Różyczka, M. & Franco, J. 1996, Toroidal magnetic fields and the evolution of wind-driven nebulae, ApJ, 469, L127

van Marle et al. 2008, submitted

van Marle, A. J., Langer, N., Achterberg, A., & García-Segura, G. 2006, Forming a constant density medium close to long gamma-ray bursts, A&A, 460, 105

van Marle, A. J., Langer, N., & García-Segura, G. 2005, Constraints on gamma-ray burst and supernova progenitors through circumstellar absorption lines, A&A, 444, 837

Villaver, E., García-Segura, G., & Manchado, A. 2002a, The dynamical evolution of the circumstellar gas around low- and intermediate-mass stars. I. The asymptotic giant branch, ApJ, 571, 880

Villaver, E., Manchado, A., & García-Segura, G. 2002b, The dynamical evolution of the circumstellar gas around low- and intermediate-mass stars. II. The planetary nebula formation, ApJ, 581, 1204

Weaver, R., McCray, R., Castor, J., Shapiro, P., & Moore, R. 1977, Interstellar bubbles. II - Structure and evolution, ApJ 218, 377